Electronic Supplementary Material (ESI) for Journal of Materials Chemistry A.
This journal is © The Royal Society of Chemistry 2016

Supporting Information

Novel Aramid Nanofiber-Coated Polypropylene Separators for Lithium Ion Batteries

Shengyu Hu,[a,b,c,d] Shudong Lin,[a,b,c,d] Yuanyuan Tu,[a,c,d] Jiwen Hu*,[a,b,c,d] Yan Wu,[a,b,c]

Guojun Liu,[a,b,e] Fei Li,[a,b,c,d] FamengYu,[a,b,c] and Tingting Jiang[a,b,c]

[a] *Guangzhou Institute of Chemistry, Chinese Academy of Sciences, Guangzhou, P. R. China, 510650*

[b] *University of Chinese Academy of Sciences, No.19A, Yuquan Road, Beijing, P. R. China, 100049*

[c] *Key Laboratory of Cellulose and Lignocellulosics Chemistry, Chinese Academy of Sciences, P. R. China, 510650*

[d] *Guangdong Provincial Key Laboratory of Organic Polymer Materials for Electronics, P. R. China, 510650*

[e] *Department of Chemistry, Queen's University, 90 Bader Lane, Kingston, Ontario, Canada K7L 3N6*

More Experimental and Characterization Details

Fourier Transform Infrared (FT-IR) Spectroscopy. FT-IR spectra of the pristine PP separator and the modified separators (including PDA-PP separator, surface cationized separator and the ANFs coated separators) were recorded using a Bruker TENSOR27 FT-IR Spectrometer with a wavenumber resolution of 1 cm^{-1}.

X-ray Photoelectron Spectrometer (XPS). The elemental compositions of the pristine PP separator, the modified separators and Kevlar 49 yarn were traced via XPS (Thermo Scientific™ K-Alpha™+, Thermo Fisher Scientific Inc.) with a takeoff angle at 45°. Spectra of all of the samples were recorded using X-ray generated by an Al anode (1486.6 eV) at a power of 300 W. For survey scan from the range of 0~1000 eV, the acquisition time was set at 2 min and swept with a pass energy of 100 eV. High resolution core level XPS spectra of C and O were recorded with a pass energy of 30 eV. XPS data were treated with the advantage software package (version 5.0, Acresso

*Corresponding author: Prof. Jiwen Hu, fax: +86 20 85232307, email: hjw@gic.ac.cn

Software Inc.) provided by the equipment supplier. Core level XPS of C and O were deconvoluted to several Gaussian peaks corresponding to different chemical states.

Abrasion Tests. To evaluate the stability between the coated ANF layer and the PP porous separator, the ANF-coated separator was subjected to abrasion tests performed with a BGD 528 universal abrasion tester (Biuged Laboratory Instruments (Guangzhou) Co., Ltd., Guangzhou, China). The ANF-coated separator with dimensions of 50.0 mm × 70.0 mm (TD×MD) was attached to the sample stage with double sided adhesive tape. The sample stage was then screwed to the abrasion tester. Imperial™ Wetrodry™ 401Q polishing paper (3M Company, USA) was used as an abrasion substrate and fixed onto the back board. A counterweight was loaded to balance the sample stage, cantilever and other accessories of the tester before a 0.5 kg weight was applied onto the sample. The sample stage was then driven by an electricmotor and reciprocated on the polishing paper. The maximum stroke for the sample stage was 90.0mm. Small sections of samples of the ANF-coated separator that had been subjected to a 40 cycle of the abrasion test were washed with ethanol and acetone, before they were attached to the AFM sample stage and their surface morphologies were observed via AFM and compared with those of the pristine PP separator and to an ANF-coated separator that had not been subjected to the abrasion test. The surface roughness including the root mean-square roughness ($\boldsymbol{R}_q$) and arithmetic mean roughness ($\boldsymbol{R}_a$) of the samples before and after they were subjected to abrasion tests were calculated from Equations (1) and (2):

$$R_q = \sqrt{\frac{1}{N^2}\sum_{i=1}^{N}\sum_{j=1}^{N}(Z_{ij} - Z_{av})^2} \quad (1)$$

$$R_a = \frac{1}{N}\sum_{i=1}^{N}\sum_{j=1}^{N}|Z_{ij} - Z_{cp}| \quad (2)$$

The specific definitions of *N, i, j, Z_{ij}, Z_{av}* and Z_{cp} can be found in Wang's paper.[S1] The $\boldsymbol{R}_a$ and $\boldsymbol{R}_q$ values were obtained from calculations using the AFM software. The surface morphologies of the ANF-coated separator before and after heating at 170 °C were also carefully investigated by AFM and compared with the morphologies of pristine PP separator before and after heating treatment.

Electrolyte Durability Test. The stability of the ANF coating layer in electrolyte was also evaluated. The 0.005 wt% ANFs-PP (6) separator was stored in electrolyte (1mol·L^{-1} $LiPF_6$ in DMC:

EC: PC = 2:1:1 by weight) for one month, then removed and thoroughly rinsed with dimethyl carbonate (DMC) in order to remove the residual electrolyte. The separator was finally dried in a vacuum oven for 4 h. The treated separator was then observed by AFM and its surface morphology was compared with that of a pristine PP separator as well as that of a freshly prepared ANF-coated separator.

Mercury Intrusion Porosimetry (MIP). Porosities and pore sizes distributions of the pristine PP separator, the PDA-PP separator, the 0.005 wt% ANFs-PP (1) separator and the 0.005 wt% ANFs-PP (6) separator were characterized using a Micrometrics® Autopore IV 9500 series (Micromeritics Instrument Corporation, Norcross, USA.) system. All measurements were carried out over the pressure range 0.1 to 60000 psi. The pore diameters were determined by intrusion and extrusion of mercury and calculated from the Laplace equation (3):

$$R = -\frac{2\gamma\cos\theta}{\Delta P} \qquad (3)$$

Wherein, $\boldsymbol{R}$ is the pore diameter of the separator, $\boldsymbol{\gamma}$ is the surface tension of mercury which equals 480×10^{-5} N·cm^{-1}, $\boldsymbol{\theta}$ is the mercury contact angle to the separator and equals 130° for all samples, and $\boldsymbol{P}$ represents the applied pressure.[S2]

Mechanical Properties. Tensile strengths on the MD of the pristine PP separator and modified separators were tested using an auto tensile testing machine (Model: YL-1109, Yuelian Testing Machine Co, Ltd., Dongguan, China). Samples were trimmed into 40.0 mm×10.0 mm (MD×TD) strips and fixed with two clamps. The gauge length between the clamps was set to 15 mm. The samples were stretched with a rate of 5.0 mm/min at 30 °C.

Ionic conductivity measurements. Ionic conductivities of the pristine PP separator, the PDA-PP separator and the 0.005% ANFs-PP (6) separator were determined by sandwiching these

three kinds of separators between two stainless steel blocking electrodes (diameter: 1.6 cm), respectively. Nyquist plots in the frequency range of 0.1 Hz to 1 MHz were obtained with a perturbation amplitude of 5 mV using a Solartron 1255 frequency response analyzer in combination with a Solartron 1287 electrochemical interface. The ionic conductivity **σ** of the separator was calculated from the equation (4):

$$\sigma = \frac{d}{R_b \times S} \qquad (4)$$

Wherein, ***d*** is the thickness of the separator which equals to 2.0×10^{-4} cm for all separators because the polydopamine layer as well as the ANFs coated layer were very thin (less than 1 μm), $\boldsymbol{R}_b$ is the bulk resistances of the separator and was obtained from the Nyquist plots, ***S*** is the area of the separator (2.0 cm^2 for all samples). [S11-S12]

Electrolyte uptake. A preweighted separator was immersed in the electrolyte solution (1mol·L^{-1} $LiPF_6$ in DMC: EC: PC = 2:1:1 by weight) for 24h and then took out, excess electrolyte was wiped off. The electrolyte uptake of the separator was determined by equation (5):

$$Electrolyte\ uptake = \frac{W_2 - W_1}{W_1} \times 100\% \qquad (5)$$

Wherein, W_1 and W_2 indicate the weights of the separators before and after saturated with the liquid electrolyte.[S2]

Water contact angle (WCA) measurements. The WAC was obtained with a contact goniometer JC2000D1 (Powereach Digital Technology equipment Co. Ltd. in Shanghai, China) by the drop-shape method. The reported value was the average of 3 measurements of a water droplet locating at different positions of the separator.

More Results

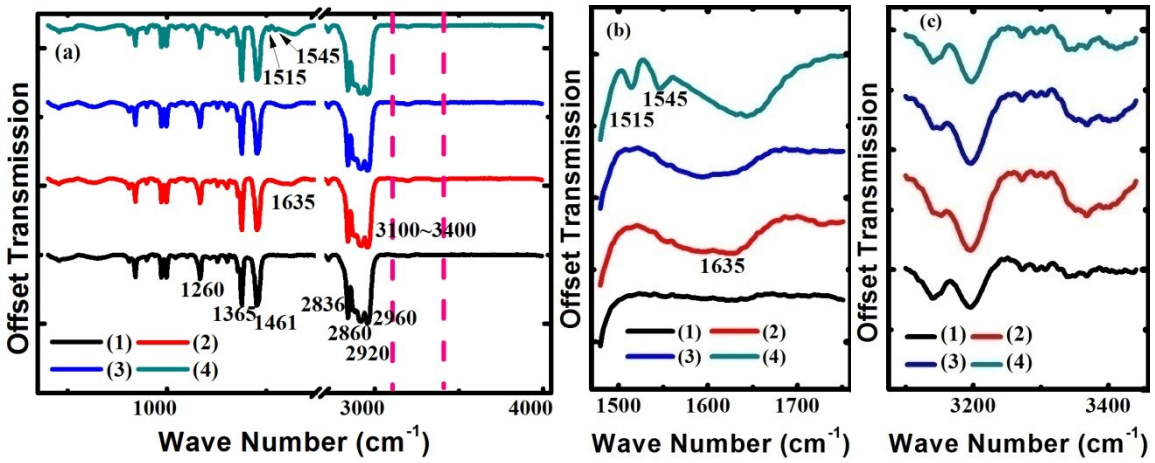

Figure S1. FT-IR spectra (a) of the pristine PP separator (line 1), the PDA-PP separator (line 2), the surface cationized PP separator (line 3) and the 0.02 wt% ANFs-PP (1) separator (line 4). Images (b) and (c) show the enlarged spectra in the absorption ranges corresponding to the stretching vibrations of carbonyl groups and hydroxyl groups, respectively.

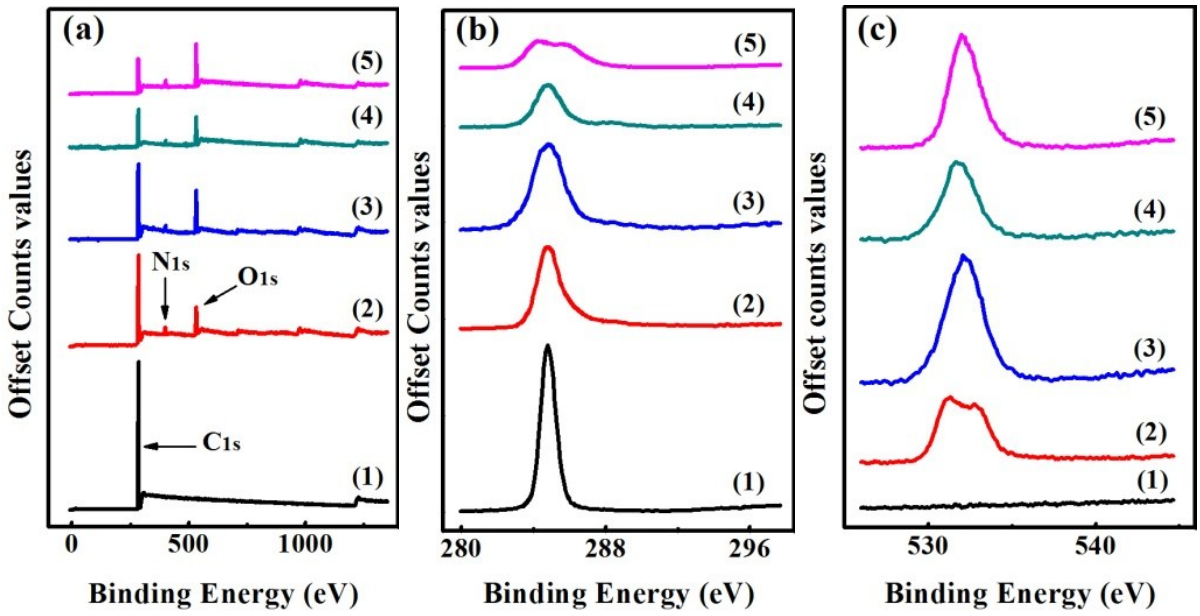

Figure S2. Survey scan XPS (a), and high resolution C (b) and O (c) core level XPS plots of the pristine PP separator (line 1, shown in black), the PDA-PP separator (line 2, shown in red), the surface cationized PP separator (line 3, shown in blue), the 0.02 wt% ANFs-PP (1) separator (line 4, shown in green), and of Kevlar yarn (line 5, shown in purple).

Table S1. Atomic percentages of C, O, and N of the pristine PP separator, the PDA-PP separator, the surface cationized PP separator, the 0.02 wt% ANFs-PP (1) separator and the Kevlar yarn.

samples	%C	%N	%O	N/C	O/C
theoretical*					
Dopamine	72.73	9.09	18.18	12.50	25.00
Kevlar yarn	77.80	11.10	11.10	14.27	14.27
Experimental*					
Pristine PP separator	100.00	—	—	—	—
PDA-PP separator	80.13	4.92	14.95	0.06	18.66
Surface cationized PP separator	81.57	0.72	17.70	0.88×10^{-3}	21.70
0.02 wt% ANFs-PP (1) separator	77.58	1.38	21.04	0.18×10^{-2}	21.12
Kevlar yarn	71.63	1.43	26.94	0.20×10^{-2}	37.61

*Note: Hydrogen is excluded because it was not detected by XPS.

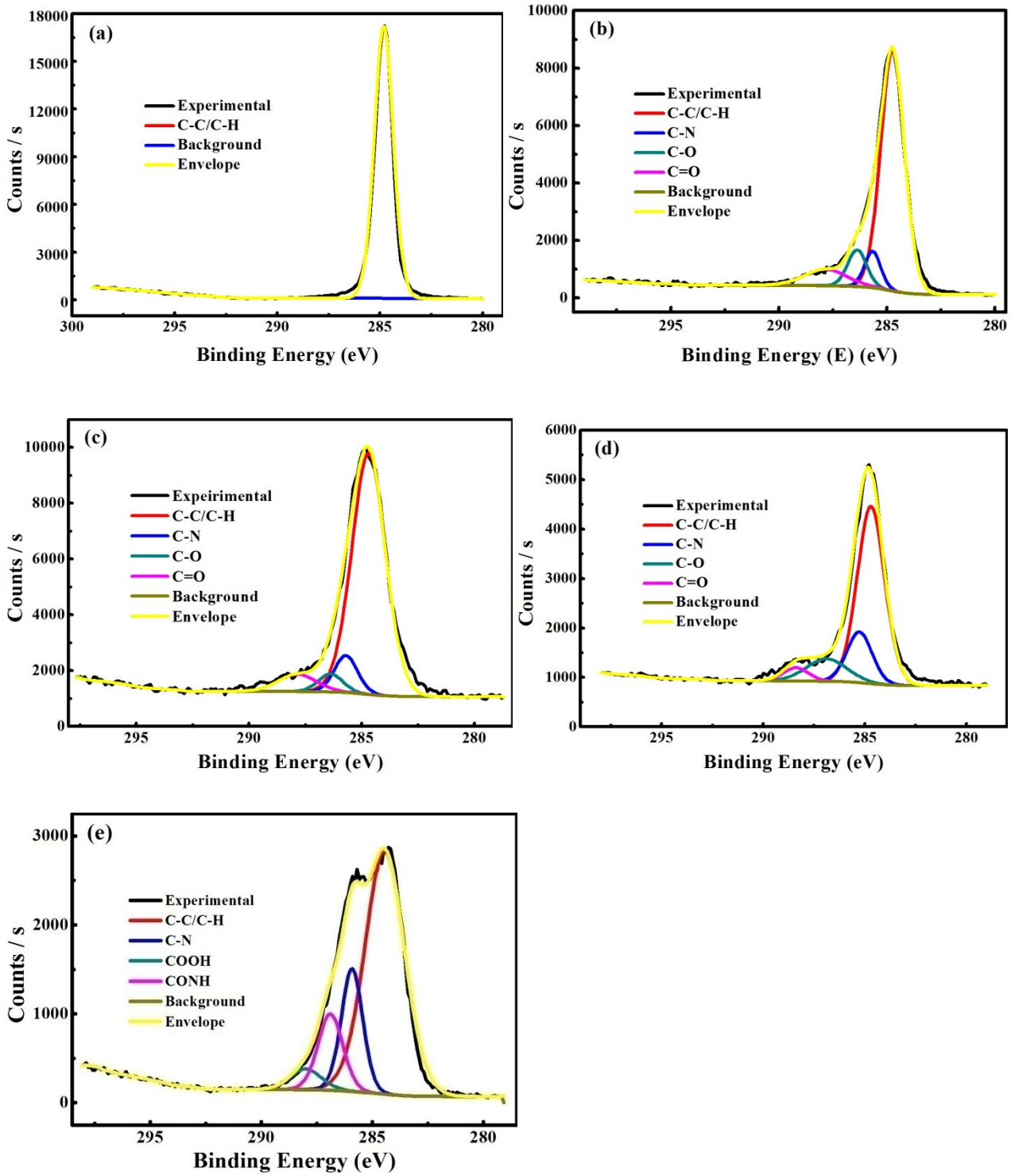

Figure S3. High resolution C_{1s} Core level XPS and fitted Gaussian peaks corresponding to different chemical states of the pristine PP separator (a), the PDA-PP separator (b), the surface cationized PP separator (c), the 0.02 wt% ANFs-PP(1) separator (d) and the aramid yarn (e).

Table S2. Peak-fitting details the pristine PP separator, the PDA-PP separator, the surface cationized PP separator, the 0.02wt% ANFs-PP (1) separator and the aramid yarn.

Sample	Chemical states	Peak BE*(eV)	FWHM(eV)	Fit Area (CPS.eV)	Atomic (%)
Pristine PP separator	C-C/C-H	284.81	1.07	19889.11	100.00
PDA-PP separator	C-C/C-H	284.74	1.28	11673.02	73.99
	C-N	285.67	0.88	1208.85	7.67
	C-O	286.38	1.03	1438.92	9.13
	C=O	287.84	2.32	1449.57	9.21
Surface cationized PP separator	C-C/C-H	284.69	1.75	16387.16	80.28
	C-N	285.70	1.22	1754.52	8.60
	C-O	286.38	1.28	910.00	4.46
	C=O	287.84	2.01	1356.04	6.66
0.02wt% ANFs-PP (1) separator	C-C/C-H	284.70	1.59	6166.24	65.64
	C-N	285.26	1.46	1629.37	17.35
	CONH	286.88	2.33	1163.87	12.41
	COOH	288.38	1.46	431.95	4.61
Aramid yarn	C-C/C-H	284.44	2.08	6182.34	64.98
	C-N	285.91	1.13	1696.92	17.85
	CONH	286.88	1.30	1213.09	12.77
	COOH	288.00	1.66	417.90	4.40

***Note:** the fit peak bonding energy is referred to reference [S3~S10] with fine adjustments to achieve the best fitting curves.

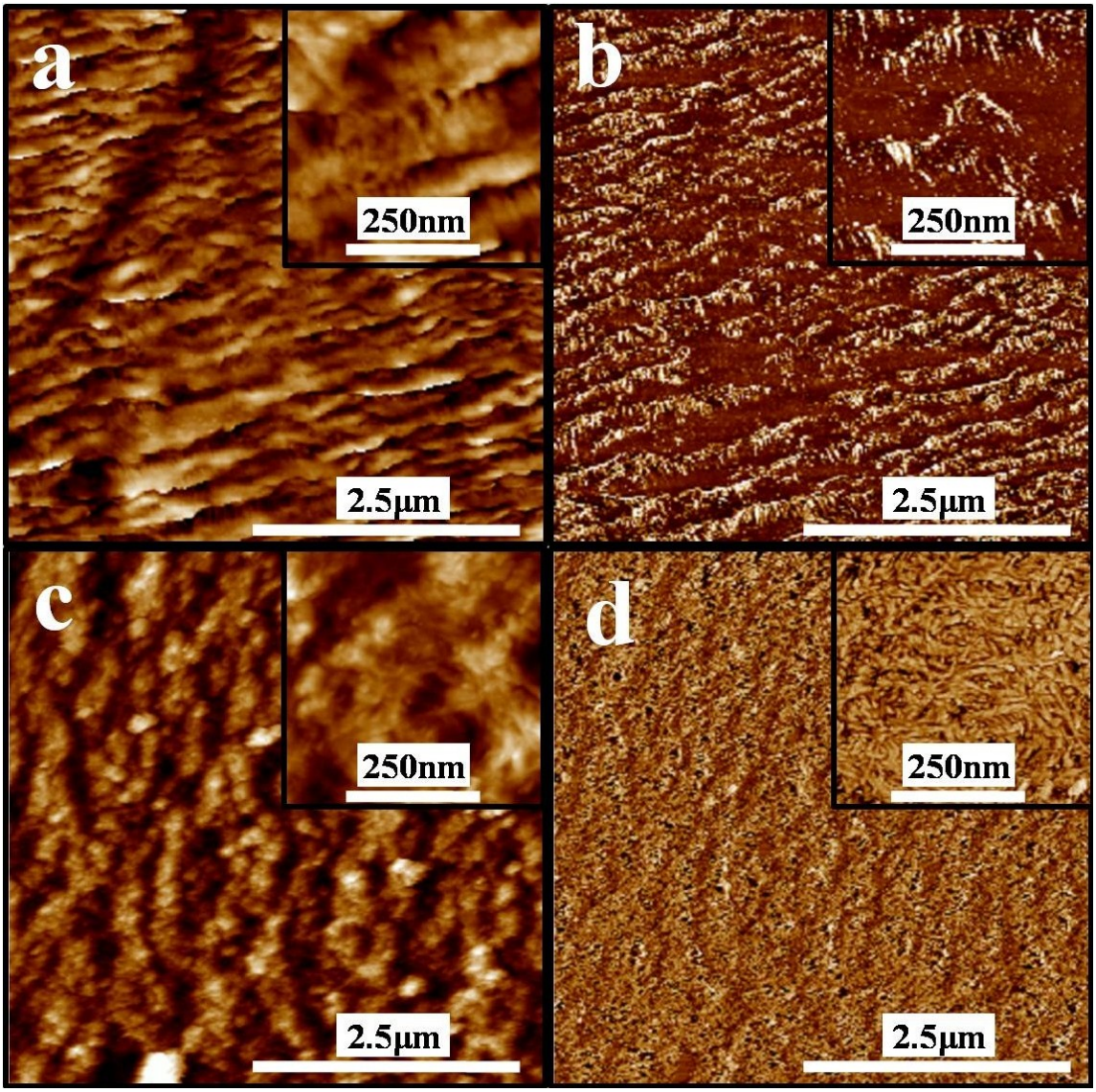

Figure S4. AFM Height image of the 0.02 wt% ANFs-PP (1) separator after the abrasion test (a) and storage in electrolyte (1 mol·L^{-1} $LiPF_6$ in DMC:EC:PC = 2:1:1 by weight) for 1 month (c). (b) and (d) are the corresponding phase images of (a) and (c), respectively.

Table S3. Surface roughness analysis results of the pristine PP separator, the as prepared 0.02 wt% ANFs-PP (1) separator and of this latter separator after abrasion tests and storage in electrolyte for 1 month.

Surface roughness	Pristine PP separator	0.02 wt% ANFs-PP (1) separator		
		As prepared	After abrasion test	After stored in electrolyte for 1 month
R_q* (nm)	25.5	21.9	18.4	21.3
R_a* (nm)	20.4	17.6	14.7	17.2

***Note:** the R_q and R_a values were calculated from the whole images of **Figure 2h**, **Figure S4a** and **Figure S4c**. Results were calculated using the AFM software.

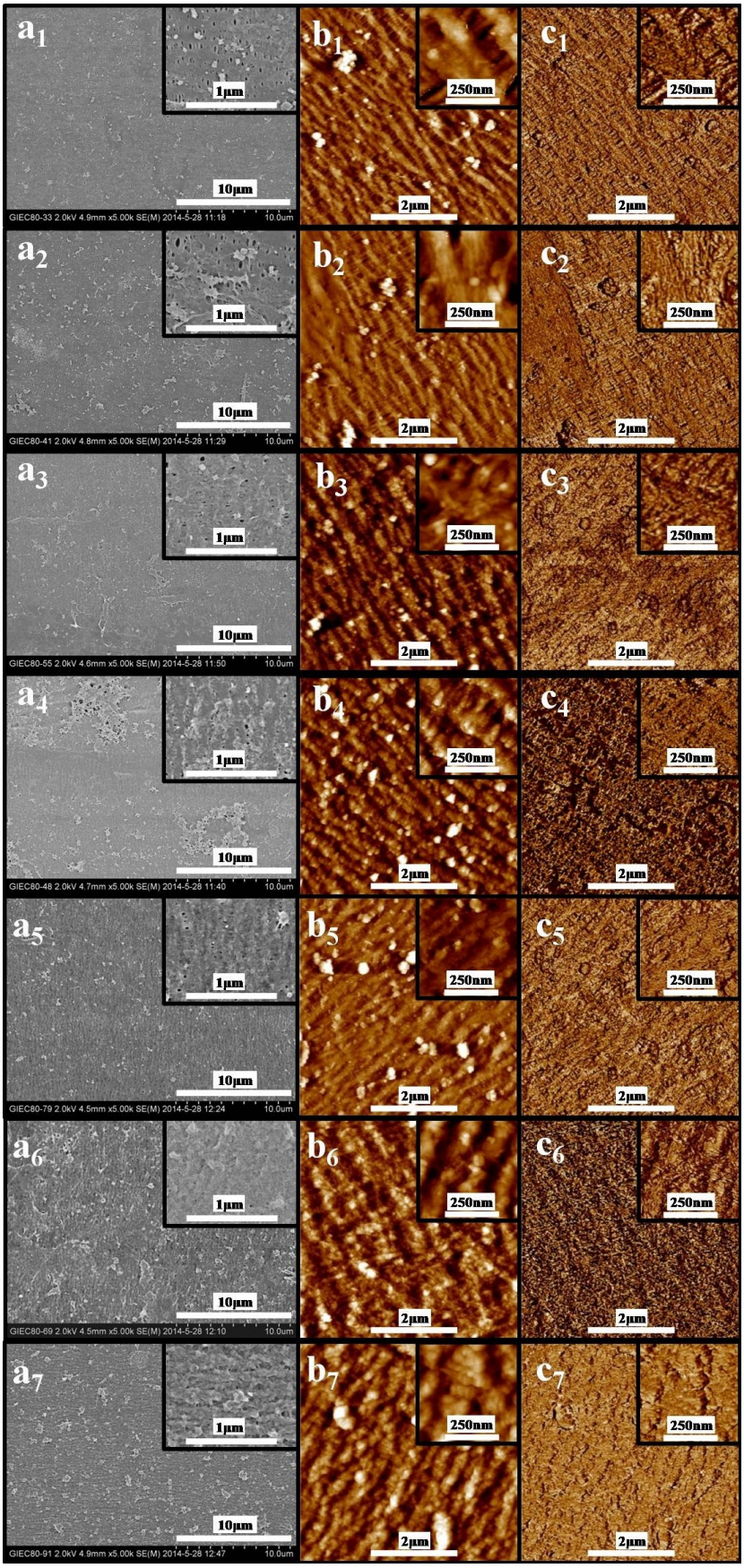

Figure S5. SEM images (a_1)~(a_7) the ANF-coated separators with 1 ~ 7 layers of ANFs on both sides of the separator when the concentration of the ANF dispersion was kept at 0.005 wt%. Images (b_1)~(b_7) and (c_1)~(c_7) are corresponding AFM height and phase topographies of (a_1)~(a_7), respectively.

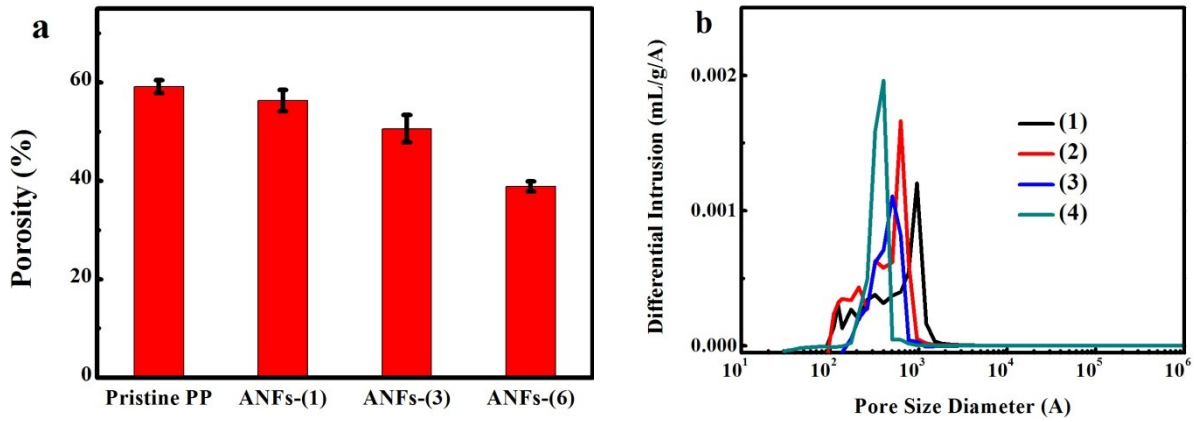

Figure S6. Porosity (a) and pores size distribution (b) of the pristine PP separator (line 1, shown in black), the 0.005 wt% ANFs-PP (1) separator (line 2, shown in red), the 0.005 wt% ANFs-PP (3) separator (line 3, shown in blue) and the 0.005 wt% ANFs-PP (6) separator (line 4, shown in green).

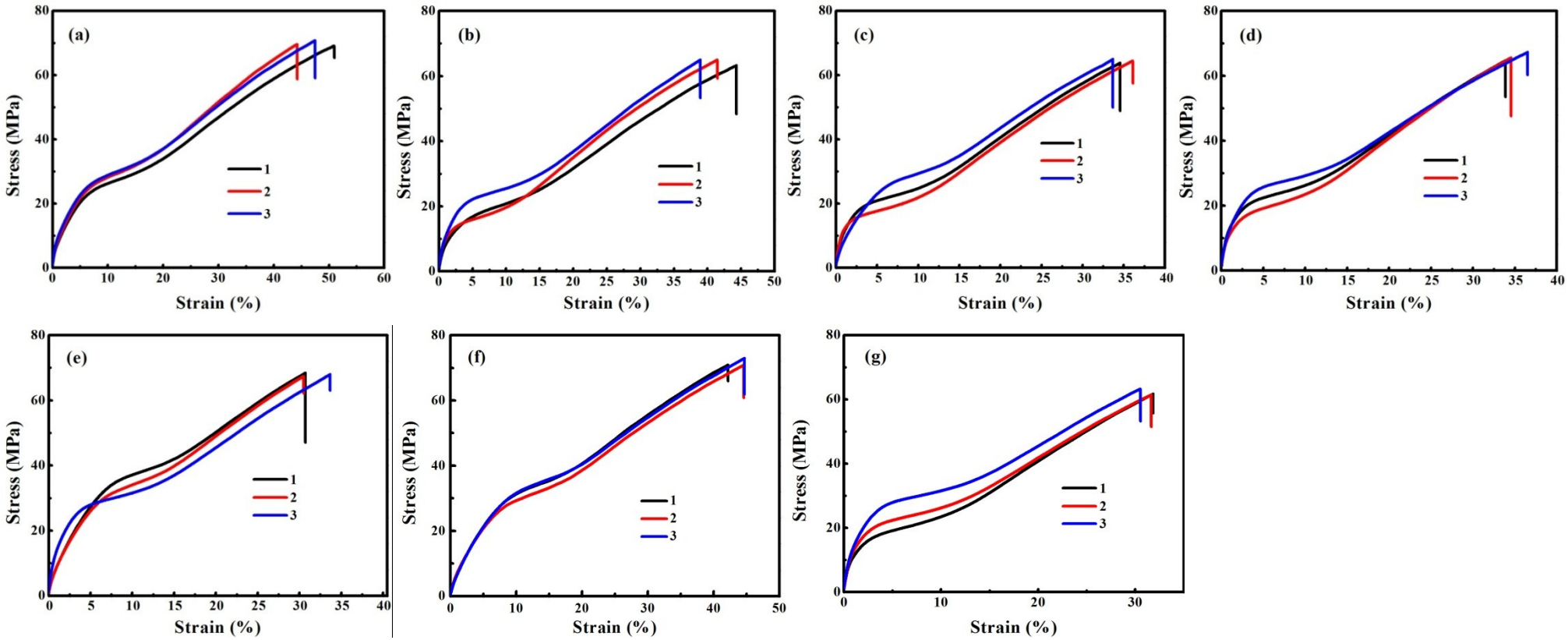

Figure S7. Stress-Strain curves in the machine direction (MD) of the pristine PP separator (a), the PDA-PP separator (b), the 0.005 wt% ANFs-PP (1) separator (c), the 0.005 wt% ANFs-PP (3) separator (d), the 0.005 wt% ANFs-PP (6) separator (e), the PP separators treated in the Tris-HCl buffer without dopamine (f) and the PP separators treated with dopamine for 24 h (g). Each plot includes three different measurements for the same kind of separator.

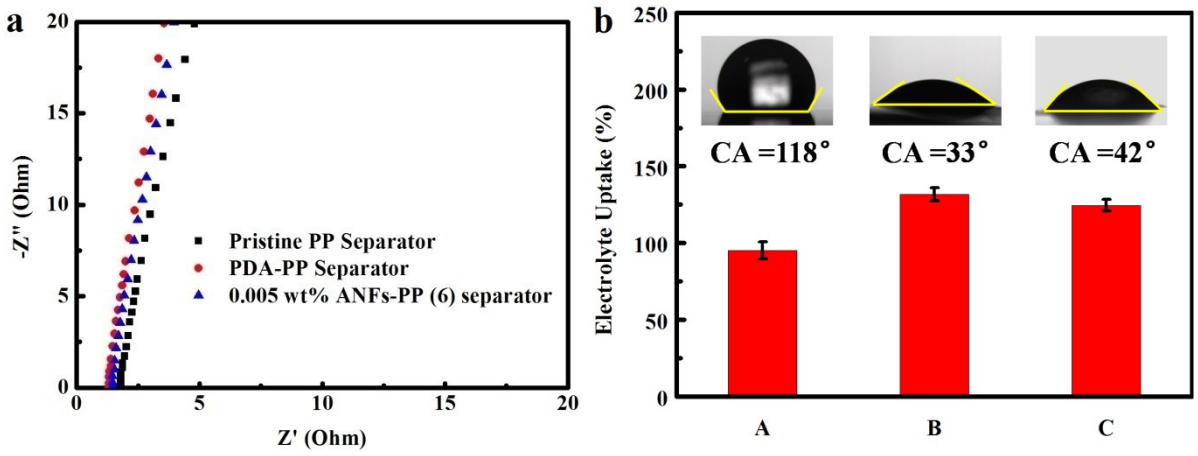

Figure S8. Nyquist plots of the cells (stainless steel/separator/stainless steel) employing the liquid electrolyte-soaked pristine PP separator, the PDA-PP separator and the 0.005 wt% ANF-PP (6) separator (a). The obtained bulk resistance $\boldsymbol{R}_b$ (intercept of Z' axis) of the pristine PP separator, the PDA-PP separator and the 0.005wt% ANF-PP (6) separator is 1.79 Ω, 1.32 Ω and 1.45 Ω, respectively. Figure (b) is the electrolyte uptake of the separators (A: the pristine PP separator; B: PDA-PP separator; C: the 0.005 wt% ANFs-PP (6) separator), insert is the water contact angle of the corresponding separator.

Reference

[S1] J. Wang, P. Chen, H. Li, B. Wang, C. Zhang and N. Ren, *Surf. Interface Anal.*, 2008, **40**, 1299–1303.

[S2] P. Arora and Z. J. Zhang, *Chem. Rev.*, 2004, **104**, 4419-4462.

[S3] B. Li, J. Gao, X. Wang, C. Fan, H. Wang and X. Liu, *Appl. Surf. Sci.*, 2014, **290**, 137-141.

[S4] R. A. Zangmeister, T. A. Morris and M. J. Tarlov, *Langmuir*, 2013, **29**, 8619-8628.

[S5] L. Q. Xu, W. J. Yang, K.-G. Neoh, E.-T. Kang and G. D. Fu, *Macromolecules*, 2010, **43**, 8336-8339.

[S6] M. Su, A. Gu, G. Liang and L. Yuan, *Appl. Surf. Sci.*, 2011, **257**, 3158-3167.

[S7] T. Peng, R. Cai, C. Chen, F. Wang, X. Liu, B. Wang and J. Xu, *J. Macromol. Sci. (B),* 2012, **51**, 538-550.

[S8] M. Widodo, Plasma Surface Modification of Polyaramid Fibers for Protective Clothing, Doctor degree thesis, North Carolina State Universty, 2011, p. 261.

[S9] J. Wang, P. Chen, H. Li, W. Li, B. Wang, C. Zhang and R. Ni, *Surf. Interface Anal.*, 2008, **40**, 1299-1303.

[S10] M. Su, A. Gu, G. Liang and L. Yuan, *Appl. Surf. Sci.*, 2011, **257**, 3158-3167.

[S11] Y. Zhu, F. Wang, L. Liu, S. Xiao, Z. Chang, Y. Wu, *Energy Environ. Sci.*, 2013, **6**, 618-624.

[S12] Z. Zhang, Y. Lai, Z. Zhang, K. Zhang and J. Li, *Electrochim. Acta*, 2014, **129**, 55-61.